Charge-Transfer Interaction of Methyl Viologen with Zeolite Framework and Dramatic Blue Shift of Methyl Viologen−Arene Charge-Transfer Band upon Increasing the Size of Alkali Metal Cation

Y. S. Park, S. Y. Um, and K. B. Yoon*

Contribution from the Department of Chemistry, Sogang University, Seoul 121-742, Korea

Received March 17, 1998. Revised Manuscript Received December 22, 1998

Abstract: A series of alkali metal-exchanged zeolites X and Y co-exchanged with small amounts (1 per unit cell) of methyl viologen (MV^{2+}) were prepared. The diffuse reflectance UV−vis spectra of the dried zeolites showed broad absorption bands in the 220−320-nm region. Decomposition of the bands revealed that each absorption band consists of two Gaussian bands. Of the two, the one that appears at the higher energy region is always more intense and much broader than the other that appears at the lower energy region. The broader, higher energy band (BHEB) progressively red-shifted upon increasing the electropositivity of the alkali metal cation, while the narrower, lower energy band (NLEB) remained stationary. The BHEB was assigned as the charge-transfer (CT) band between MV^{2+} and the zeolite framework on the basis of the linear relationship established between the energy of the absorption maximum and Sanderson's partial charge of the framework oxygen. The remaining, stationary NLEB was consequently assigned as the absorption band of MV^{2+} in the zeolite media. Subsequent formation of CT complexes of MV^{2+} with guest arene donors such as anthracene, 1-methoxynaphthalene, and pentamethylbenzene within the zeolites showed a dramatic blue shift of MV^{2+}−arene CT bands upon increasing the size of alkali metal cation. The possible reasons for the dramatic, cation-dependent spectral shift of MV^{2+}−arene CT bands are discussed.

Introduction

The cations in zeolites have been known to play important roles other than merely compensating the negative charges in the framework.[1−20] Most notably, it has been shown that they sensitively govern the donor strength of the zeolite framework.[5−18] Zeoilte Y, for instance, normally behaves as an acid catalyst in various reactions with Na^+ as the countercation. However, it can be readily switched to a base catalyst by replacing Na^+ with Cs^+.[16−18] Thus, mere replacement of a common alkali metal cation with another can dramatically change the donor strength (basicity) of the zeolite framework.

The donor strength of the framework has been demonstrated to increase upon increasing the electropositivity of the cation.[1−22] The results from the XPS studies of the zeolite framework,[6−9] the FT-IR studies of various probe molecules,[10−14] and the UV−vis measurements of iodine adsorbed on various zeolites[15] have

(1) (a) Breck, D. W. *Zeolite Molecular Sieves*; Wiley: New York, 1974. (b) Barrer, R. M. *Zeolites and Clay Minerals as Sorbents and Molecular Sieves*; Academic: London, 1978.

(2) (a) Chen, N. Y.; Garwood, W. E.; Dwyer, F. G. *Shape-Selective Catalysis in Industrial Applications*; Marcel Dekker: New York, 1989. (b) Csicsery, S. M. In *Zeolites Chemistry and Catalysis*; Rabo, J. A., Ed.; ACS Monograph 171; American Chemical Society: Washington, DC, 1976; p 680 ff. (c) Weisz, P. B.; Frilette, V. Z. *J. Phys. Chem.* **1960**, *64*, 382.

(3) Ruthven, D. M. *Principles of Adsorption and Adsorption Process*; Wiley: New York, 1984.

(4) (a) Rabo, J. A.; Angell, C. L.; Kasai, P. H.; Schomaker, V. *Discuss. Faraday Soc.* **1966**, *41*, 328. (b) Kasai, P. H.; Bishop, R. J., Jr. *J. Phys. Chem.* **1973**, *77*, 2308.

(5) (a) Mortier, W. J.; Schoonheydt, R. A. *Prog. Solid State Chem.* **1985**, *16*, 1. (b) Mortier, W. J. *J. Catal.* **1978**, *55*, 138. (c) Heidler, R.; Janssens, G. O. A.; Mortier, W. J.; Schoonheydt, R. A. *J. Phys. Chem.* **1996**, *100*, 19728. (d) Van Genechten, K. A.; Mortier, W. J. *Zeolites* **1988**, *8*, 273.

(6) (a) Barr, T. L.; Lishka, M. A. *J. Am. Chem. Soc.* **1986**, *108*, 3178. (b) Barr, T. L.; Chen, L. M.; Mohsenian, M.; Lishka, M. A. *J. Am. Chem. Soc.* **1988**, *110*, 7962. (c) Barr, T. L. *Zeolites* **1990**, *10*, 760.

(7) Okamoto, Y.; Ogawa, M.; Maezawa, A.; Imanaka, T. *J. Catal.* **1988**, *112*, 427.

(8) (a) Huang, M.; Adnot, A.; Kaliaguine, S. *J. Am. Chem. Soc.* **1992**, *114*, 10005. (b) Huang, M.; Adnot, A.; Kaliaguine, S. *J. Catal.* **1992**, *137*, 322.

(9) Kaushik, V. K.; Bhat, S. G. T.; Corbin, D. R. *Zeolites* **1993**, *13*, 671.

(10) (a) Barthomeuf, D. *J. Phys. Chem.* **1984**, *88*, 42. (b) Barthomeuf, D. *Stud. Surf. Sci. Catal.* **1991**, *65*, 157. (c) Murphy, D. Massiani, P.; Franck, R.; Barthomeuf, D. *J. Phys. Chem.* **1996**, *100*, 6731.

(11) Huang, M.; Kaliaguine, S. *J. Chem. Soc., Faraday Trans.* **1992**, *88*, 751.

(12) (a) Barthomeuf, D.; Ha, B.-H. *J. Chem. Soc., Faraday Trans.* **1973**, *69*, 2158. (b) de Mallmann, A.; Barthomeuf, D. *Zeolites* **1988**, *8*, 292. (c) de Mallmann, A.; Barthomeuf, D. *J. Phys. Chem.* **1989**, *93*, 5636. (d) Dzwigaj, S.; de Mallmann, A.; Barthomeuf, D. *J. Chem. Soc., Faraday Trans.* **1990**, *86*, 431.

(13) Uytterhoeven, L.; Dompas, D.; Mortier, W. J. *J. Chem. Soc., Faraday Trans.* **1992**, *88*, 2753.

(14) (a) Mirodatos, C.; Pichat, P.; Barthomeuf, D. *J. Phys. Chem.* **1976**, *80*, 1335. (b) Mirodatos, C.; Abou Kais, A.; Vedrine, J. C.; Pichat, P.; Barthomeuf, D. *J. Phys. Chem.* **1976**, *80*, 2366.

(15) Choi, S. Y.; Park, Y. S.; Hong, S. B.; Yoon, K. B. *J. Am. Chem. Soc.* **1996**, *118*, 9377.

(16) Yashima, T.; Sato, K.; Hayasaka, T.; Hara, N. *J. Catal.* **1972**, *26*, 303.

(17) Ono, Y. *Stud. Surf. Sci. Catal.* **1980**, *5*, 19.

(18) (a) Hattori, H. *Chem. Rev.* **1995**, *95*, 537. (b) Tanabe, K.; Misono, M.; Ono, Y.; Hattori, H. *Stud. Surf. Sci. Catal.* **1989**, *51*, 1.

(19) (a) Vinek, H.; Noller, H.; Ebel, M.; Schwarz, K. *J. Chem. Soc., Faraday Trans. 1* **1977**, *73*, 734. (b) Klading, W.; Noller, H. *J. Catal.* **1973**, *29*, 385.

(20) Mochida, I.; Yoneda, Y. *J. Org. Chem.* **1968**, *33*, 2161.

(21) Other important factors that govern the physicochemical properties of zeolites are the Si/Al ratio and the method of pretreatment.

(22) Dyer, A. *An Introduction to Zeolite Molecular Sieves*; Wiley: New York, 1988.

10.1021/ja980912p CCC: $18.00
Published on Web 03/19/1999

served as the experimental bases in establishing the above fact. Sanderson's electronegativity equalization principle has served as a theoretical basis to correlate the experimentally observed donor strength of the framework and the calculated partial charge of the framework oxygen.[5]

Now the question is, how do cations affect the donor strength of the framework? Surprisingly however, only a limited number of studies have addressed this crucial question, although the answer to it is quite essential for deepening our understanding of zeolites for various practical applications. Nevertheless, Mortier's[5] and Jhon's[23] groups proposed a charge-transfer (CT) interaction between the cation and the framework in order to account for the progressive increase of the zeolite donor strength upon increasing the size of the cation on the basis of theoretical studies. However, direct experimental confirmation based on Mulliken's CT theory has not yet been attempted.[24]

Stemming from our interests in the CT reactions within zeolites,[25] we have carried out a systematic study aimed at experimentally elucidating the possible CT nature of the cation−framework interaction by employing the well-known bipyridinium acceptor, methyl viologen (MV^{2+}, *N*,*N*′-dimethyl-4,4′-bipyridinium), as the probe cation and zeolites X and Y as the prototypical zeolites.

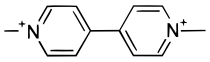

MV^{2+}

This paper reports the CT interaction between MV^{2+} and zeolite framework and the dramatic spectral shift of the intrazeolite MV^{2+}−arene CT complexes upon varying the size of the alkali metal cation.

Experimental Section

Materials. Na^+X (Linde 13X, Lot No. 120307) and Na^+Y (LZY-52, Lot No. 968087061020-S) were purchased from Strem and Union Carbide, respectively. ZSM-5, with the Si/Al ratio of 150, was a gift from ALSI−PENTA Zeolite GmbH. Nafion film was a kind gift from Professor Woon-kie Paik. Methyl viologen dichloride ($MVCl_2$) from Hannong Chemical Co. was recrystallized repeatedly until colorless. $MV(PF_6)_2$ was obtained by metathesis of $MVCl_2$ with NH_4PF_6 in water. The obtained PF_6^- salt was recrystallized repeatedly using acetonitrile and ethyl acetate. $MVBr_2$ was obtained by metathesis of $MV(PF_6)_2$ and $(n\text{-Bu})_4NBr$ in acetonitrile. The iodide (I^-) and triflate (trifluoromethanesulfonate, OTf^-) salts of MV^{2+} were obtained by reaction of 4,4′-bipyridine with iodomethane and methyl trifluoromethanesulfonate, respectively, in methanol. The arene donors were purchased from Aldrich and purified according to the standard procedures.[26] *n*-Hexane was treated with concentrated sulfuric acid prior to distillation from sodium under an argon atmosphere. The distilled solvent was subsequently kept in a Schlenk flask in a glovebox charged with high-purity argon.

Ion Exchange. The Na^+ forms of zeolites X and Y were treated with aqueous 1 M NaCl solution once again and subsequently washed with distilled deionized water (>18 MΩ) until the silver ion test for chloride was negative. The Li^+ and K^+ forms of zeolites X and Y were obtained from the corresponding Na^+-exchanged zeolites using standard aqueous ion-exchange methods. The Rb^+- and Cs^+-exchanged zeolites X and Y were prepared similarly from the corresponding K^+ forms. Despite repetition of the exchange procedures five times, elemental analyses of the final zeolites revealed incomplete exchange, as shown in Table 1.

Table 1. Chemical Compositions of the Alkali Metal-Exchanged Zeolites X and Y Used in This Study

zeolite	unit cell composition
Li^+Y	$Li_{37}Na_{16}Al_{53}Si_{139}O_{384}$
Na^+Y	$Na_{53}Al_{53}Si_{139}O_{384}$
K^+Y	$K_{49}Na_4Al_{53}Si_{139}O_{384}$
Rb^+Y	$Rb_{35}K_{13}Na_2H_3Al_{53}Si_{139}O_{384}$
Cs^+Y	$Cs_{37}K_{14}Na_2Al_{53}Si_{139}O_{384}$
Li^+X	$Li_{68}Na_{16}Al_{84}Si_{108}O_{384}$
Na^+X	$Na_{84}Al_{84}Si_{108}O_{384}$
K^+X	$K_{75}Na_9Al_{84}Si_{108}O_{384}$
Rb^+X	$Rb_{51}K_{21}Na_5H_7Al_{84}Si_{108}O_{384}$
Cs^+X	$Cs_{46}K_{26}Na_6H_6Al_{84}Si_{108}O_{384}$

The incorporation of MV^{2+} into various alkali metal-exchanged zeolites was carried out by aqueous ion exchange of M^+ with MV^{2+} using $MVCl_2$. The amount of MV^{2+} in the doped zeolites was controlled to be approximately 1 per unit cell (8 supercages). The unexchanged amount of MV^{2+} ion in the wash was quantified by UV−vis spectrophotometry monitored at $\lambda = 257$ nm ($\epsilon = 20\,417$).[27] All the MV^{2+}-doped zeolites were dried in the air at ambient temperatures. The air-dried zeolites were then briefly washed with methanol prior to subsequent evacuation ($<10^{-5}$ Torr) at room temperature for 2 h.[28] The dehydration temperatures were then slowly increased to 150 and 200 °C for zeolites X and Y, respectively.[29] The samples were then evacuated at the final temperatures for an additional period of 20 h. The dried zeolites were transferred to a glovebox charged with high-purity argon and kept in tightly capped glass containers.

Nafion film was treated with hydrogen peroxide in sulfuric acid until colorless. The colorless H^+ form of the film was titrated with the hydroxide of Li^+, Na^+, or K^+, respectively, to obtain the corresponding alkali metal-exchanged film. Controlled amounts of MV^{2+} (3.4 mmol/g) were exchanged into the films by stirring them in aqueous solutions of $MVCl_2$.

Formation of Intrazeolite MV^{2+}−Arene CT Complexes. Typically, a vial containing a slurry of the dried zeolite (0.3 g) and rigorously dried *n*-hexane (5 mL) was treated with an arene donor (0.3 mmol) in the glovebox. Distinctive colors slowly developed after addition of aromatic donors to the colorless, white powders of MV^{2+}-doped zeolites. The slurry was gently shaken for a few minutes and kept in the dark for 15 h. The zeolite powders were recovered by filtration and washing with an additional 5-mL aliquot of *n*-hexane. The colored zeolites were briefly evacuated at ambient temperatures in the glovebox to remove *n*-hexane.

Spectral Measurements. An aliquot (0.25 g) of each dried, MV^{2+}-doped zeolite powder was transferred in the glovebox into a flat, cylindrical quartz cell capped with a grease stopper for the diffuse reflectance UV−vis spectral measurements. The spectra of the colored zeolites containing MV^{2+}−arene CT complexes were similarly obtained. After each measurement, the dry powder was taken out of the cell onto a watch glass in the atmosphere, and moisturization of the dry samples was carried out by deliberately spraying them with a water aerosol. The colored zeolites incorporating the CT complexes of MV^{2+} and ring-methylated arene donors ($Ar\text{-}CH_3$) were placed in the dry state under a fluorescent light in order to photoinduce color change. For comparison, the colored samples were also irradiated using a 500-W Hg lamp at wavelengths longer than 400 nm. The spectral change was monitored occasionally. An alumina disk was used as the reference for obtaining

(23) No, K. T.; Chon, H.; Ree, T.; Jhon, M. S. *J. Phys. Chem.* **1981**, *85*, 2065.

(24) (a) Mulliken, R. S. *J. Am. Chem. Soc.* **1950**, *72*, 601. (b) Mulliken, R. S.; Person, W. B. *Molecular Complexes*; Wiley: New York, 1969. (c) Mulliken, R. S.; Person, W. B. *Molecular Complexes: A Lecture and Reprint Volume*; Wiley: New York, 1969.

(25) (a) Yoon, K. B. *Chem. Rev.* **1993**, *93*, 321. (b) Yoon, K. B.; Kochi, J. K. *J. Am. Chem. Soc.* **1989**, *111*, 1128. (c) Yoon, K. B.; Kochi, J. K. *J. Phys. Chem.* **1991**, *95*, 1348. (d) Yoon, K. B.; Kochi, J. K. *J. Phys. Chem.* **1991**, *95*, 3780. (e) Yoon, K. B.; Huh, T. J.; Corbin, D. R.; Kochi, J. K. *J. Phys. Chem.* **1993**, *97*, 6492. (f) Yoon, K. B.; Huh, T. J.; Kochi, J. K. *J. Phys. Chem.* **1995**, *99*, 7042.

(26) Perrin, D. D.; Armarego, W. L. F. *Purification of Laboratory Chemicals*, 3rd ed.; Pergamon: Oxford, 1988.

(27) Summers, L. A. *The Bipyridinium Herbicides*; Academic: New York, 1980.

(28) The brief washing of the air-dried zeolites with the more volatile methanol prior to evacuation was intended to facilitate the dehydration since the final temperatures were not high enough to complete dehydration.

(29) MV^{2+} was not stable above the final temperatures.

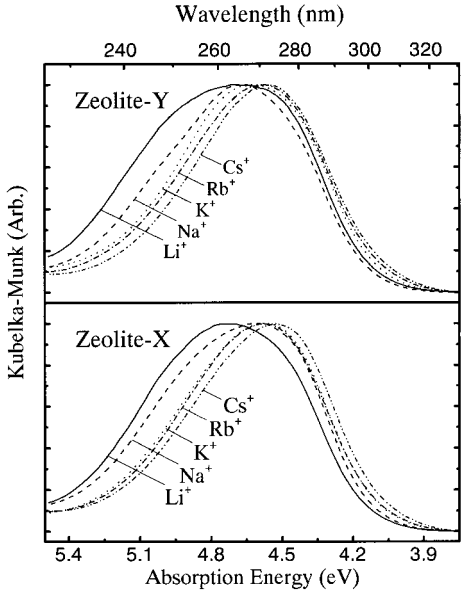

Figure 1. Diffuse reflectance UV−vis spectra of the dehydrated $MV^{2-}-M^+Y$ (top) and $MV^{2+}-M^+X$ (bottom).

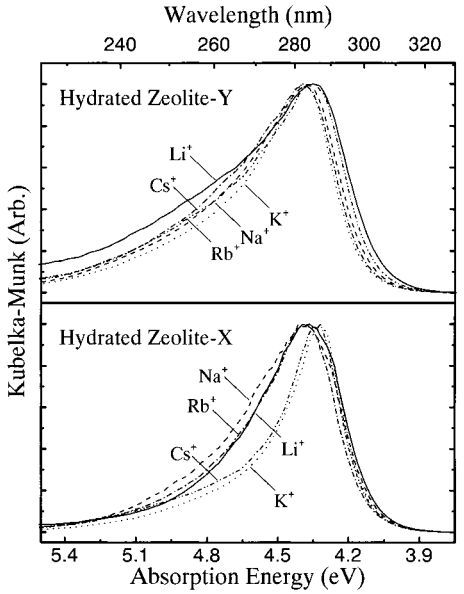

Figure 2. Diffuse reflectance UV−vis spectra of the fully hydrated $MV^{2+}-M^+Y$ (top) and $MV^{2+}-M^+X$ (bottom).

the backgrounds of the zeolite samples. The dried, finely ground NaCl powder contained in the cylindrical quartz cell was used as the reference for MV^{2+} salts with various anions. The MV^{2+} salts were diluted with dry NaCl powder by grinding them in the glovebox.

Instrumentation. The diffuse reflectance UV−vis spectra of the colored zeolites were recorded on a Shimadzu UV-3101PC (0.1 nm resolution) equipped with an integrating sphere. The X-band ESR spectra of the green zeolites were obtained from a Bruker ER 200E-SRC spectrometer. The compositions of the alkali metal-exchanged zeolites were analyzed at Galbraith Laboratories Inc. or the Analytical Laboratory of the Korea Institute of Science and Technology.

Results

Table 1 lists the chemical compositions of various alkali metal-exchanged zeolites used in this study. For convenience, the alkali metal-exchanged zeolites X and Y are hereafter denoted as M^+X and M^+Y, respectively, where M^+ stands for the alkali metal ion, i.e., Li^+, Na^+, K^+, Rb^+, or Cs^+. The corresponding MV^{2+}-doped zeolites are denoted as $MV^{2+}-M^+X$ and $MV^{2+}-M^+Y$, respectively. The reason for the minimal exchange of MV^{2+} into each M^+X and M^+Y (1 per unit cell or per 8 supercages) was to not significantly alter the donor strength of the zeolite framework after incorporation of MV^{2+}. Thus, M^+ remained as the major cation and MV^{2+} became the minor, probe cation.

Diffuse Reflectance UV−Vis Spectra of the MV^{2+}-Doped M^+Y and M^+X. The diffuse reflectance UV−vis spectra of the dried, $MV^{2+}-M^+Y$ and $MV^{2+}-M^+X$ samples showed absorption bands in the 220−320-nm region, as shown in Figure 1.[30] Most notably, the absorption bands progressively red-shifted upon increasing the size of M^+. Thus, the absorption maximums were Li^+, 264; Na^+, 265; K^+, 268; Rb^+, 271; and Cs^+, 272 for $MV^{2+}-M^+Y$, and Li^+, 261; Na^+, 268; K^+; 270; Rb^+, 272; and Cs^+, 274 for $MV^{2+}-M^+X$ (in nm). Concomitantly, the bandwidths of the spectra progressively decreased upon increasing the size of M^+, the order being $Li^+ > Na^+ > K^+ > Rb^+ > Cs^+$. Scrutiny of the spectra revealed that this phenomenon actually arises from the progressive red shift of the higher energy fronts (220−270-nm region), while the lower energy fronts (270−320-nm region) of the spectra remained nearly stationary. A closer look of the lower energy fronts further revealed that they also generally shift to red, although in small increments, upon replacing M^+ with the more electropositive ones.

In marked contrast, the fully hydrated samples gave nearly the same absorption maximums, as shown in Figure 2. Thus, no such aspect of the cation-dependent progressive shift was observed from the fully hydrated samples. In addition, all the absorption bands turned sharper with nearly the same bandwidth irrespective of M^+. It is, however, interesting to note that all the bands show long residual absorption over the higher energy region.

Decomposition of the Spectra. Even a glimpse of the spectra of the dried MV^{2+}-doped zeolites in Figure 1 immediately shows that they are not single Gaussian bands. The decomposition of the spectra using multiple Gaussian bands revealed that each absorption band best fits with a long, weak tail band and two full Gaussian bands, as typically shown for $MV^{2+}-M^+Y$ in Figure 3. The weak tail band (dotted line) was assigned as the residual absorption of the zeolite framework.

Of the two Gaussian bands, the one that appears at the higher energy region (dashed curve) is always much broader (fwhm = ∼0.68 eV) and more intense than the one (fwhm = ∼0.43 eV) that appears at the lower energy region (dash−dotted curve). Moreover, the broader, higher energy band (BHEB) progressively red-shifted upon increasing the electropositivity of the surrounding alkali metal ion (M^+), i.e., 256 (Li^+), 258 (Na^+), 263 (K^+), 265 (Rb^+), and 268 nm (Cs^+), while the narrower, lower energy band (NLEB) remained stationary at 278 nm. Similarly, the observed BHEBs for $MV^{2+}-M^+X$ were 259 (Li^+), 261 (Na^+), 265 (K^+), 266 (Rb^+), and 268 nm (Cs^+), with fwhm = ∼0.68 eV, while NLEB remained stationary at 279 nm, with fwhm = ∼0.36 eV.

Linear Relationship of the BHEB with the Framework Donor Strength. Since the increase in the electropositivity of the countercation gives rise to the increase in the donor strength (basicity) of the framework (see Introduction), the relationship between the spectral shift of BHEB and the framework donor strength was examined. For this purpose, it is, in fact, necessary to get the ionization potentials of zeolite frameworks, $I_p(Z)$, as the direct measures of the framework donor strengths as in the case of small molecules. However, the corresponding values

(30) Since the wavelength scale is not linear in energy, the spectra are presented in an energy scale (eV) in the abscissa. For comparison, the wavelength scale (nm) is also marked at the top of the figure.

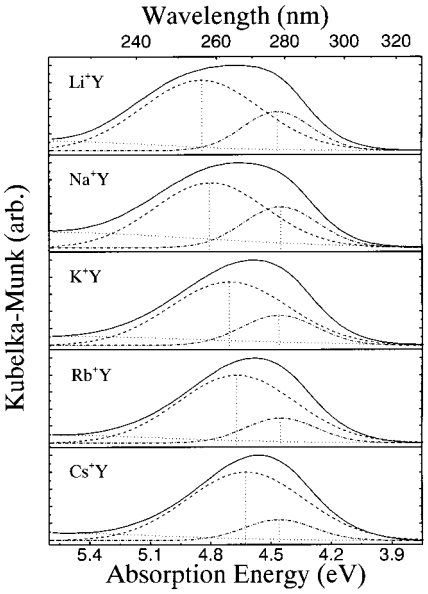

Figure 3. Decomposed spectra of the dehydrated $MV^{2+}-M^{+}Y$ for five different alkali metal cations (as indicated), showing the residual absorption of the zeolite framework (···), the broader, higher energy band, BHEB (- - -), and the narrower, lower energy band, NLEB (−·−).

of $I_p(Z)$ are not available at this stage for zeolites X and Y, although $I_p(Z)$ for NaZSM-5 has been estimated to be higher than 11.4 eV by Trifunac et al.[31]

Instead, we used Sanderson's partial charges of the framework oxygen atoms as viable measures for the framework donor strengths since they have been shown to be linearly correlated with the experimentally observed framework donor strengths. Sanderson's partial charges of the framework oxygen atoms for the MV^{2+}-doped zeolites were calculated on the basis of their chemical compositions listed in Table 1. Here, the perturbation of the partial charges caused by the replacement of two alkali metal ions with one MV^{2+} was neglected.[32]

An excellent linear relationship resulted, as shown in Figure 4 for both zeolites. This led us to conclude that the progressive red shift of BHEB indeed arises in response to the increase in the negative charge density of the framework oxygen, i.e., upon increasing the framework donor strength. Since this relationship complies with Mulliken's CT theory,[24] the BHEBs were assigned as the corresponding CT bands between MV^{2+} and the negatively charged frameworks.

The linear relationship shown in Figure 4 was formulated as the following:

$$h\nu_{CT} = 1.7(\delta_o)_X + 5.3 \quad (1)$$

$$h\nu_{CT} = 4.2(\delta_o)_Y + 5.9 \quad (2)$$

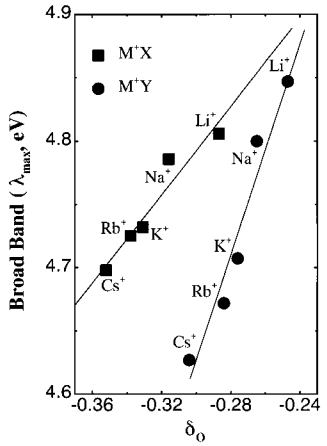

Figure 4. Linear relationship between the BHEB in Figure 3 and the calculated Sanderson's (average) partial charge of the framework oxygen of $M^{+}Y$ and $M^{+}X$ (as indicated).

where $h\nu_{CT}$ represents the energy of the $MV^{2+}-$framewrok CT band (BHEB) at the absorption maximum, and $(\delta_o)_X$ and $(\delta_o)_Y$ represent the average charge densities of the framework oxygen atoms in zeolites X and Y, respectively. The obtained slope was significantly larger for zeolite Y (4.2) than that of zeolite X (1.7). However, the obtained offset values were not much different, being 5.3 and 5.9 for $M^{+}X$ and $M^{+}Y$, respectively.

Formation of Framework−MV^{2+}−Arene Triad Complexes. Since MV^{2+} is well known to form highly colored CT complexes with various arene donors within the restricted confinements of zeolites,[25] we subsequently incorporated some prototypical arene donors into $MV^{2+}-M^{+}X$ and $MV^{2+}-M^{+}Y$ in order to investigate the effect of the surrounding alkali metal ion on the $MV^{2+}-$arene CT complexes. Knowing that MV^{2+} forms a CT complex with the framework as described in the previous section, the intended intrazeolite $MV^{2+}-$arene CT complexes should more strictly be formulated as a triad (donor−acceptor−donor) interaction of MV^{2+} with both the framework (donor 1) and the arene (donor 2) according to the following scheme:

$$\underset{\text{donor 1}}{\text{framework}} - \underset{\text{acceptor}}{MV^{2+}} - \underset{\text{donor 2}}{\text{arene}}$$

The prototypical arene donors selected for this purpose were pentamethylbenzene (PMB), 1-methoxynaphthalene (1-MeO-NAPH), and anthracene (ANT). These arene donors have been known to form yellow, orange, and purple CT complexes, respectively, with MV^{2+} in $Na^{+}Y$.[25]

Upon addition of arene donors, the colorless, MV^{2+}-doped zeolites slowly developed characteristic CT colors due to formation of $MV^{2+}-$arene complexes within the supercages. Although the intensities of the CT colors were somewhat low due to there being only small amounts of MV^{2+} in the zeolites, the obtained colors were distinctive enough to be differentiated. The resultant $MV^{2+}-$arene CT colors progressively blue-shifted upon increasing the size of M^{+} on going from Li^{+} to Cs^{+}.[33] Consistent with the gradual color change, the obtained diffuse reflectance UV−vis spectra revealed the progressively blue-shifting aspect of the $MV^{2+}-$arene CT band upon increasing the size of M^{+}, as typically demonstrated in Figure 5 for zeolite Y.

(31) (a) Werst, D. W.; Tartakovsky, E. E.; Piocos, E. A.; Trifunac, A. D. *J. Phys. Chem.* **1994**, *98*, 10249. (b) Piocos, E. A.; Werst, D. W.; Trifunac, A. D.; Eriksson, L. A. *J. Phys. Chem.* **1996**, *100*, 8408.

(32) Sanderson's intermediate electronegativity, S_z, of each M^{+}-exchanged zeolite was calculated according to the equation, $S_z = (S_M{}^p S_{Si}{}^q S_{Al}{}^r S_O{}^t)^{1/(p+q+r+t)}$, where, S_M, S_{Si}, S_{Al}, and S_O represent Sanderson's electronegativities of the alkali metal cation, silicon, aluminum, and oxygen, respectively, and p, q, r, and t represent the number of the corresponding element, respectively, in a unit cell. The corresponding Sanderson's (average) partial charge of the framework oxygen, δ_o, was then obtained using the equation, $\delta_o = (S_Z - S_O)/(2.08 S_O{}^{1/2})$. Sanderson's electronegativity for each element is as follows: Si, 2.14; Al, 1.71; O, 3.65; Li, 0.89; Na, 0.56; K, 0.45; Rb, 0.31; Cs, 0.22. The values were taken from the following reference: Huheey, J. E.; Keiter, E. A.; Keiter, R. L. *Inorganic Chemistry*, 4th ed.; Harper Collins College Publications: New York, 1993; p 187 ff.

(33) For instance, the colors of $MV^{2+}-$ANT complex in $M^{+}Y$ were plum (Li^{+}), pink (Na^{+}), brownish pink (K^{+}), brown (Rb^{+}), and brownish yellow (Cs^{+}).

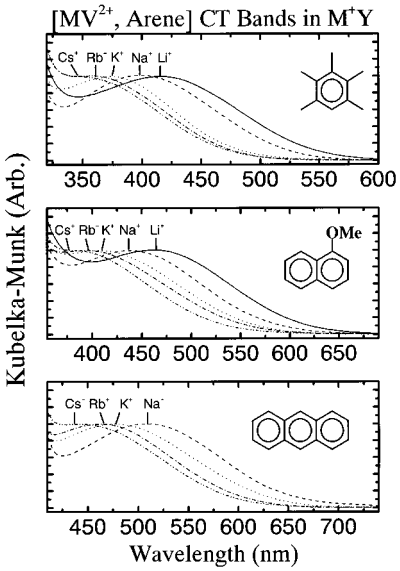

Figure 5. Progressive blue shift of the MV^{2+}−arene CT band for three prototypical arene donors (as indicated) in the dehydrated M^+Y as the size of the alkali metal cation increases.

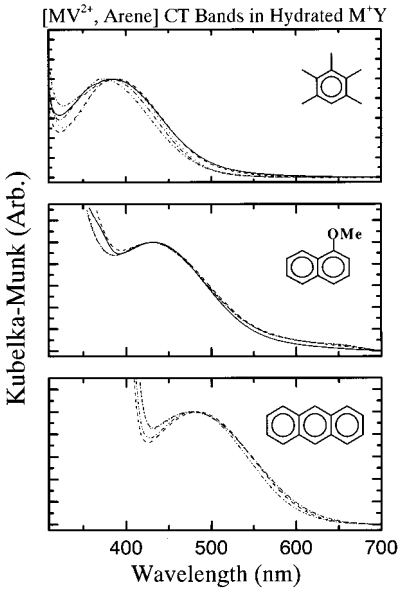

Figure 6. Convergence of the MV^{2+}−arene CT bands in Figure 5 after hydration.

In marked contrast, all the MV^{2+}−arene CT bands nearly overlapped each other irrespective of M^+, as shown in Figure 6, when the zeolites were deliberately hydrated. The CT colors of the resulting MV^{2+}−arene complexes also became nearly identical for a given arene donor.

Interestingly, a negative linear relationship was observed between the CT bands of MV^{2+}−framework and MV^{2+}−arene complexes, as illustrated in Figure 7. Thus, upon the blue shift of the MV^{2+}−arene CT band, the MV^{2+}−framework CT band red-shifted. Another point worth noticing in this figure is that the MV^{2+}−arene CT bands appear at the higher energy region in zeolite X than in zeolite Y for a given arene donor.

Formation of Anthracene Cation Radical in Li^+Y. When Li^+Y was the host for the MV^{2+}−ANT CT complex, unexpected absorption bands also appeared at 570, 660, and 720 nm in addition to the corresponding CT band at ~500 nm. These extra bands also appeared when ANT was adsorbed on plain

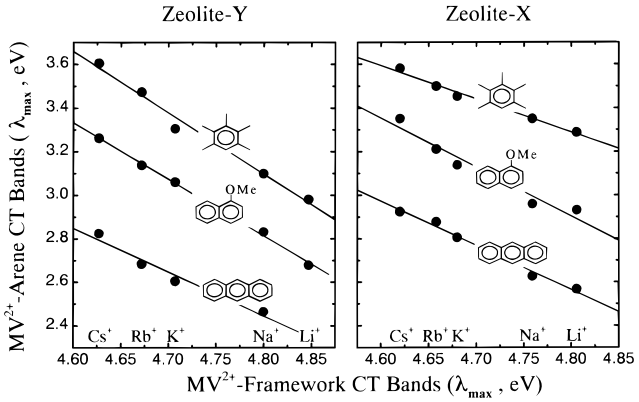

Figure 7. Negative linear relationship established between the MV^{2+}−framework and MV^{2+}−arene CT bands for three prototypical arene donors (as indicated) in zeolites Y (left) and X (right).

Li^+Y undoped with MV^{2+}. These extra bands were assigned as those of anthracene cation radical $ANT^{\bullet+}$ from the direct comparison of the bands with those of authentic[34] $ANT^{\bullet+}$ independently generated in Ca^{2+}-exchanged zeolite Y ($Ca^{2+}Y$).[35] This phenomenon did not occur with poorer arene donors such as 1-MeO-NAPH and PMB and in other alkali metal-exchanged zeolites tested in this study. Due to the interference by $ANT^{\bullet+}$, the precise absorption maximum of the MV^{2+}−ANT CT band in Li^+Y could not be obtained (see the missing point in Figures 5 and 7).

Generation of $MV^{\bullet+}$ from MV^{2+}−PMB CT Complex in M^+X ($M^+ = K^+$, Rb^+, Cs^+) by CT Excitation. The MV^{2+}−PMB complex gives various shades of yellow color within M^+-exchanged zeolites X and Y. The yellow color of the MV^{2+}−PMB CT complex, however, tended to turned green after several hours of exposure to room light when the complex was assembled within M^+X with $M^+ = K^+$, Rb^+, and Cs^+. The green coloration occurred almost immediately when the samples were deliberately irradiated at the CT band ($\lambda > 400$ nm) using a more intense 500-W Hg lamp. The diffuse reflectance UV−vis spectra of the green samples revealed the presence of the characteristic blue bands of $MV^{\bullet+}$ at 570, 610, 665, and 733 nm,[36] in addition to the broad yellow CT band, as shown in Figure 8. The ESR spectrometry of the green zeolite samples showed an isotropic signal at $g = 2.003$, characteristic of $MV^{\bullet+}$ in zeolite media.[36]

$MV^{\bullet+}$ was also generated in Cs^+Y and Na^+X when the encapsulated MV^{2+}−PMB complex was irradiated using the more intense Hg lamp. However, the resulting intensities of $MV^{\bullet+}$ were weaker in these zeolites than in M^+X ($M^+ = K^+$, Rb^+, Cs^+). The photoinduced generation of $MV^{\bullet+}$ also readily occurred with other ring-methylated arene donors ($Ar\text{-}CH_3$) such as mesitylene, durene, prehnitene, and methylnaphthalene. In strong contrast, formation of $MV^{\bullet+}$ did not occur from the CT complexes with methyl-free arene donors or in the complete absence of any arene donor.

(34) Shida, T. *Electronic Absorption Spectra of Radical Ions*; Elsevier: Amsterdam, 1988.

(35) (a) Stamires, D. N.; Turkevich, J. *J. Am. Chem. Soc*. **1964**, *86*, 749. (b) Hirschler, A. E.; Neikam, W. C.; Barmby, D. S.; James, R. L. *J. Catal*. **1965**, *4*, 628. (c) Edlund, O.; Kinell, P.-O.; Lund, A.; Shimizu, A. *J. Chem. Phys*. **1967**, *46*, 3679. (d) Kurita, Y.; Sonoda, T.; Sato, M. *J. Catal*. **1970**, *19*, 82. (e) Corio, P. L.; Shih, S. *J. Catal*. **1970**, *18*, 126. (f) Shih, S. *J. Phys. Chem*. **1975**, *79*, 2201. (g) Xu, T.; Haw, J. F. *J. Am. Chem. Soc*. **1994**, *116*, 10188. (h) Werst, D. W.; Tartakovscky, E. E.; Piocos, E. A.; Trifunac, A. D. *J. Phys. Chem*. **1994**, *98*, 10249.

(36) (a) Yoon, K. B.; Kochi, J. K. *J. Am. Chem. Soc*. **1988**, *110*, 6586. (b) Park, Y. S.; Um, S. Y.; Yoon, K. B. *Chem. Phys. Lett*. **1996**, *252*, 379. (c) Yoon, K. B.; Park, Y. S.; Kochi, J. K. *J. Am. Chem. Soc*. **1996**, *118*, 12710.

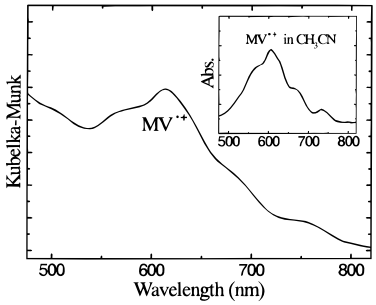

Figure 8. Generation of $MV^{\bullet+}$ from the MV^{2+}−PMB CT complex assembled in the basic M^+X ($M^+ = K^+$, Rb^+, Cs^+) after exposure to room light for several hours or direct irradiation of the CT band ($\lambda >$ 400 nm) using a 500-W Hg lamp for 10 min. The inset shows the authentic spectrum of $MV^{\bullet+}$ in CH_3CN.

Discussion

The Aspect of the BHEB as the CT Band. The relatively large bandwidth of the BHEB accords well with the general aspect of the CT bands being broad.[24] The CT band (BHEB) being more intense than the local band (NLEB) in Figure 3 is akin to that of iodine.[15,37,38] The sharp disappearance of the BHEBs upon hydrating the dried MV^{2+}-doped zeolites shown in Figure 2 should be attributed to the loss of direct interaction between MV^{2+} and the framework by the intervening water, since water is known to strongly adsorb on the polar oxide surface of zeolites. Subsequently, the intervening water is likely to eliminate the direct interaction between the organic acceptor and the framework.[25f] This result further emphasizes the importance of direct contact between MV^{2+} and the framework to give the corresponding CT band (BHEB).

However, the persistent residual absorption of the fully hydrated samples toward the higher region in Figure 2 suggests that the CT interaction between MV^{2+} and the framework does not vanish completely, even in the fully hydrated states. This may reflect that a small portion of MV^{2+} acceptors can retain direct contact with the zeolite framework, even in the fully hydrated states, presumably due to the limited space of the supercage.

The Use of Sanderson's Partial Charge of the Framework Oxygen. According to Mulliken's CT theory for weak intermolecular donor−acceptor complexes, the absorption maximum of the CT band ($h\nu_{CT}$) is approximately related to the ionization potential of the donor, $I_p(D)$, and the electron affinity of the acceptor, $E_a(A)$, according to the following equation:[24,39]

$$h\nu_{CT} = I_p(D) - E_a(A) + C \qquad (3)$$

where C represents a constant. More often, $E_a(A)$ has been replaced by the reduction potential of the acceptor, $E_{red}(A)$, if the former is not readily available. By the same analogy, we believe the use of Sanderson's partial charges of the framework oxygen atoms (δ_o) instead of the unavailable $I_p(Z)$ values for the zeolite frameworks is equally justified in verifying the CT nature of BHEBs in Figure 3, since δ_o values have been demonstrated to be linearly correlated with the experimentally observed basicities or donor strengths of the frameworks.[5−15] Accordingly, we believe the linear relationship established in Figure 4 and eqs 1 and 2 is viable to attest to the origin of the BHEBs with Mulliken's CT criteria.

The observed larger slope for zeolite Y (4.2) than for zeolite X (1.7) in Figure 4 is quite intriguing. This indicates that the degree of red shift of the CT band upon increasing the framework donor strength is much more sensitive for zeolite Y than zeolite X for a common acceptor, MV^{2+}. This may arise due to the increase in the number of the alkali metal cations in zeolite X supercage which intervene between the positively charged MV^{2+} and the framework. The intervening metal cations may in some way hamper the closer contact between MV^{2+} and the framework by repelling the positively charged acceptor away from the framework surface or altering the orientation of MV^{2+} with respect to the available basic site. Consistent with this interpretation, CT bands have been shown to blue-shift upon increasing the intermolecular distance[40−42] or the steric hindrance[43] between the donor−acceptor pairs. We also observed that MV^{2+} readily gives a visible (yellow) CT band with hexamethylbenzene in solution but not with hexaethylbenzene, which is a stronger donor.[44]

Alternatively, the congestion of the supercage with the increased number of M^+ in zeolite X may push MV^{2+} to the less basic sites of the framework since the basic sites are known to be inhomogeneous.[10c,5c]

No matter what the reasons, this result suggests that the cation-dependent donor strengths of the frameworks cannot be judged merely on the basis of their chemical compositions. Rather, the actual donor strength of the framework being exerted to an acceptor is more likely to depend on the structure, Si/Al ratio, size of the cation, and nature of the available basic sites in the framework. The actual donor strength exerted by the framework to the acceptor is also proposed to vary depending on the size and shape of the acceptor.[45] We believe this reasoning can be extended to the structure-dependent CT interaction of iodine with the zeolite framework described in our previous report.[15]

CT Interaction of MV^{2+} with Various Charge-Balancing Anions. It is well established that MV^{2+} forms CT complexes with various counteranions *in the solid state*.[46] The most widely studied anions are halides ($X^- = Cl^-$, Br^-, I^-) and some anionic metal complexes such as $Cu_2Cl_6^{2-}$, $MnCl_4^{2-}$, $FeCl_4^{2-}$, and $ZnCl_4^{2-}$. For example, the colors of MVX_2 are colorless (Cl^-), yellow (Br^-), and red (I^-) in the solid state. Although CT interaction between MV^{2+} and Cl^- is not visually apparent in the colorless $MVCl_2$, the diffuse reflectance spectrum of the crystal clearly shows the corresponding CT band at 377 nm in addition to the local band of MV^{2+} at 260 nm.[46a] Likewise, the CT interaction between MV^{2+} and the counteranions is believed to prevail in all the MV^{2+} salts, regardless of the type and the donor strength of the anion.

(37) (a) Benesi, H. A.; Hildebrand, J. H. *J. Am. Chem. Soc*. **1948**, *70*, 2382. (b) Benesi, H. A.; Hildebrand, J. H. *J. Am. Chem. Soc*. **1949**, *71*, 2703. (c) Hildebrand, J. H. *Science* **1965**, *150*, 3695.

(38) (a) Keefer, R. M.; Andrews, L. J. *J. Am. Chem. Soc*. **1952**, *74*, 1891. (b) Hastings, S. H.; Franklin, J. L.; Schiller, J. C.; Matsen, F. A. *J. Am. Chem. Soc*. **1953**, *75*, 2900. (c) Nagakura, S. *J. Am. Chem. Soc*. **1958**, *80*, 520.

(39) Hanna, M. W.; Lippert, J. L. In *Molecular Complexes, Vol. 1*; Foster, R., Ed.; Crane, Russak & Co.: New York, 1973.

(40) (a) Kadhim, A. H.; Offen, H. W. *J. Am. Chem. Soc*. **1967**, *89*, 1805. (b) Kadhim, A. H.; Offen, H. W. *J. Chem. Phys*. **1968**, *48*, 749.

(41) (a) Offen, H. W.; Studebaker, J. F. *J. Chem. Phys*. **1967**, *47*, 253. (b) Trotter, P. J. *J. Chem. Phys*. **1967**, *47*, 775. (c) Ewald, A. H. *Trans. Faraday Soc*. **1968**, *64*, 733.

(42) (a) Staab, H. A.; Krieger, C.; Wahl, P.; Kay, K.-Y. *Chem Ber*. **1987**, *120*, 551. (b) Bauer, H.; Briare, J.; Staab, H. A. *Angew. Chem., Int. Ed. Engl*. **1983**, *22*, 334. (c) Bauer, H.; Briare, J.; Staab, H. A. *Tetrahedron Lett*. **1985**, *26*, 6175.

(43) Rathore, R.; Lindeman, S. V.; Kochi, J. K. *J. Am. Chem. Soc*. **1997**, *119*, 9393.

(44) Park, Y. S.; Yoon, K., B., unpublished result.

(45) Jacobs, P. A.; Mortier, W. J.; Uytterhoeven, J. B. *J. Inorg. Nucl. Chem*. **1978**, *40*, 1919.

(46) (a) Nakahara, A.; Wang, J. H. *J. Phys. Chem*. **1963**, *67*, 496. (b) Haque, R.; Coshow, W. R.; Johnson, L. F. *J. Am. Chem. Soc*. **1969**, *91*, 3822. (c) Macfarlane, A. J. Williams, R. J. P. *J. Chem. Soc. A* **1969**, 1517.

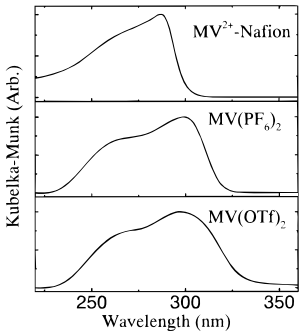

Figure 9. Diffuse reflectance spectra of MV^{2+} salts with three different anions (as indicated).

As a test case, we carefully measured the diffuse reflectance spectra of the PF_6^- and OTf^- (triflate) salts of MV^{2+} *in the solid state*. Although these anions are normally believed to be highly inert, and hence are not expected to possess any measurable donor strengths, the spectra of the colorless salts clearly revealed the presence of additional absorption bands at ~300 nm as well as the local band of MV^{2+} at ~260 nm, as shown in Figure 9. These additional absorption bands at ~300 nm were assigned as the corresponding CT bands of MV^{2+} and the counteranion from the analogy of the halide salts.

Moreover, the diffuse reflectance spectrum of MV^{2+} with Nafion (a polymer with perfluorinated polyethylene backbone and tethered vinyl ether $-CF_2-CF_2-SO_3^-$ units)[47] as the counteranion also revealed the presence of an additional band at ~280 nm as well as the local band of MV^{2+} at ~260 nm (see Figure 9, top). This additional band was similarly assigned as the corresponding CT band between MV^{2+} and the $-CF_2-SO_3^-$ units of the Nafion polymer by the same analogy of MV^{2+} and triflate ($CF_3SO_3^-$). Interestingly, the CT band blue-shifted by about 20 nm on going from triflate to Nafion. This may arise due to the steric hindrance imposed by the polymer backbone to the CT interaction between MV^{2+} and $-CF_2-SO_3^-$ unit.[48]

The overall results unambiguously demonstrate that MV^{2+} can form CT complexes with its counteranions regardless of their donor strengths, shapes, and valency. Likewise, the CT interaction between MV^{2+} and zeolite should be viewed as a normal interaction between MV^{2+} and the counteranion, where the anionic zeolite framework is just a class of polyvalent anions.

Effect of M^+ on the Spectral Shift of $MV^{2+}-$Arene CT Band. The CT band reflects the energy difference between the ground and excited states of the complex. Therefore, the progressive blue shift of the $MV^{2+}-$arene CT band upon increasing the size of M^+ should be interpreted in terms of the increase of the excited state or the decrease of the ground-state energy of the complex. Alternatively, the blue shift can arise from a simultaneous shift of the two energy states away from each other or in the same direction but with different magnitudes such that the net difference in the energy states increases.

However, it is premature at this stage to draw a solid conclusion on the progressive blue shift of the $MV^{2+}-$arene CT band upon increasing the size of M^+ since too many factors are changing upon changing the countercation. First, the degree of possible interaction between the countercation and the guest arene donors is subject to substantial change upon changing the countercation. Second, the change of the micropolarity of the supercage because of the change of the size and location of the cation is significant. Third, the steric effect imposed by the size and number of the cation is expected to be substantial, considering the relatively large sizes of MV^{2+} and arene donors in such a confined space of the supercage. Furthermore, the change of the donor strength of the framework upon changing the electropositivity of M^+ may also significantly affect the framework$-MV^{2+}-$arene triad interaction in the excited as well as in the ground states.

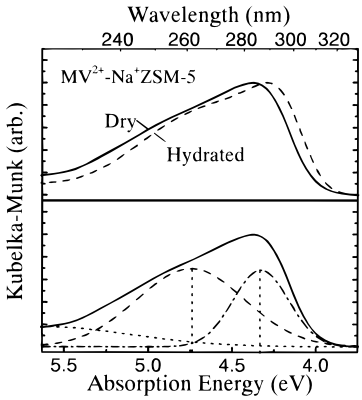

Figure 10. Diffuse reflectance UV−vis spectra of $MV^{2+}-Na^+$ZSM-5 in the dry (—) and the hydrated (- - -) states, showing the presence of BHEB at around 250 nm even before decomposition (top). Decomposition of the spectrum of the dry sample showing the corresponding BHEB and NLEB in ZSM-5 (bottom).

Overall, we believe it is rather premature at this stage to attempt to interpret the observed experimental facts. Nevertheless, it is certain that a $MV^{2+}-$arene CT complex can act as a visual probe for monitoring different alkali metal cations within zeolites X and Y.

The Behavior of NLEB. Garcia and Scaiano and their co-workers[49] have recently demonstrated that the NLEB, i.e., the local band of MV^{2+}, red-shifts upon decreasing the size of the zeolite host. Thus, the local band of MV^{2+} was reported to appear at 270 nm in Na^+Y, 280 nm in Na^+X, and 290 nm in Na^+ZSM-5. They attributed this fact to the possible changes in the polarity of the internal voids, differences in the planarity of the rings, and/or molecular orbital distortions owing to the confinement in a restricted space. Based on their result, a more pronounced separation between BHEB and NLEB was expected if ZSM-5 was employed as the host for MV^{2+}.

Indeed, as shown in Figure 10 (top), the BHEB clearly showed up as a broad shoulder band at around 250 nm, even before decomposition. The subsequent decomposition revealed BHEB and NLEB at 261 and 287 nm, respectively, with the corresponding bandwidth (fwhm) being 0.75 and 0.39 eV, respectively. This result confirmed the red-shifting behavior of the NLEB upon decreasing the pore size of the zeolite, consistent with the results of Garcia and Scaiano and their co-workers.[49] Most of all, this result demonstrated the existence of the BHEB as a shoulder band prior to decomposition.

Unlike MV^{2+}-exchanged faujasite-type zeolites (X and Y), even the fully hydrated ZSM-5 sample showed a distinguished shoulder band at ~260 nm. This indicates that water does not effectively eliminate the $MV^{2+}-$framework CT interaction in ZSM-5 as in zeolites X and Y. This may be attributed to the

(47) Brydson, J. A. *Plastics Materials*, 5th ed; Butterworth: London, 1989; p 361.

(48) Unlike zeolite, the $MV^{2+}-$Nafion CT band did not show a progressive spectral shift upon changing the alkali metal cation.

(49) They used hydrated zeolites, which, according to our results, give mostly NLEB. See: Alvaro, M.; Garcia, H.; Garcia, S.; Márquez, F.; Scaiano, J. C. *J. Phys. Chem.* **1997**, *101*, 3043. (b) Alvaro, M.; Facey, G. A.; Garcia, H.; Garcia, S.; Scaiano, J. C. *J. Phys. Chem.* **1996**, *100*, 18173.

hydrophobic nature of the ZSM pores[50] and the tighter fit of the bulky MV^{2+} ion within the narrower zeolite pores,[51] which causes the organic ion to unavoidably contact the zeolite framework.

Generation of $MV^{\bullet+}$ from MV^{2+}−Methylated Arene CT Complexes in M^+X ($M^+ = K^+$, Rb^+, Cs^+) by CT Excitation. It has been well established that MV^{2+}−arene CT complexes in NaY readily generate $MV^{\bullet+}$ and the corresponding $arene^{\bullet+}$ as the transient species upon photoexcitation of the CT bands.[25a,52] However, the transient species usually disappear within a millisecond time scale due to very rapid back electron transfer (BET) according to the following equation:

$$[MV^{2+},ArH]_{NaY} \underset{BET}{\overset{h\nu_{CT}}{\rightleftharpoons}} [MV^{\bullet+},ArH^{\bullet+}]_{NaY} \quad (4)$$

where ArH and $ArH^{\bullet+}$ denote an arene donor and its cation radical, respectively, and $[\ ]_{NaY}$ denotes the supercage of NaY. In this respect, the persistent existence of $MV^{\bullet+}$ from the CT complexes of MV^{2+} with methylated arene donors ($Ar\text{-}CH_3$) in M^+X ($M^+ = K^+$, Rb^+, Cs^+) by CT excitation is quite intriguing. This phenomenon is most likely to occur by the subsequent proton transfer from the cation radical of the methylated arene donor ($Ar\text{-}CH_3^{\bullet+}$) to the basic framework oxygen (OZO^{2-}) according to the following scheme:

$$[OZO^{2-},MV^{2+},Ar\text{-}CH_3] \underset{BET}{\overset{h\nu_{CT}}{\rightleftharpoons}} [OZO^{2-},MV^{\bullet+},Ar\text{-}CH_3^{\bullet+}] \quad (5)$$

$$[OZO^{2-},MV^{+\bullet},Ar\text{-}CH_3^{+\bullet}] \rightarrow [HOZO^{-},MV^{\bullet+},Ar\text{-}CH_2^{\bullet}] \quad (6)$$

$$[HOZO^{-},MV^{\bullet+},Ar\text{-}CH_2^{\bullet}] \rightarrow [HOZO^{-},MV^{\bullet+},{}^1/_2Ar\text{-}CH_2CH_2\text{-}Ar] \quad (7)$$

First, the CT excitation of the MV^{2+}−$Ar\text{-}CH_3$ complex converts $Ar\text{-}CH_3$ into the corresponding cation radical, $Ar\text{-}CH_3^{\bullet+}$ (eq 5). The cation radicals of the methylated arenes are known to readily transfer protons to bases since they are acidic.[53] Accordingly, if the framework is basic enough, then it can readily deprotonate $Ar\text{-}CH_3^{\bullet+}$ according to eq 6. The generated neutral benzylic radicals would then undergo various other reactions, including radical coupling to yield a biaryl compound (eq 7). Overall, $MV^{\bullet+}$ is likely to persist due to failure to undergo BET in eq 5, provided the zeolite is kept free of oxygen.

The above scheme can explain why $MV^{\bullet+}$ exists only as a transient species despite a much longer period of CT excitation when complexed with the methyl-free arene donors. For the above scheme to operate, the basicity of the framework should be strong enough to induce the deprotonation step in eq 6. Therefore, the ready formation of $MV^{\bullet+}$ only with the highly basic zeolites accords well with the above scheme. In conjunction with this, it is also interesting to note that the MV^{2+}−M^+X zeolites with $M^+ = K^+$, Rb^+, and Cs^+ usually turn blue when they were dehydrated at temperatures higher than 150 °C. This is likely to occur by the thermal electron transfer from the framework to MV^{2+}.

We hope the results described in this paper provide insight into the cation-dependent variation of the framework donor strength and shed light on the design and utilization of various heterogeneous electron-transfer systems organized within zeolites where MV^{2+} is employed as an electron acceptor or a mediating agent.[52,54−63]

Acknowledgment. We thank the Korea Science and Engineering Foundation (KOSEF) for supporting this work through the Aimed Basic Research Program (97-05-01-04-01-3) and the Center for Molecular Catalysis (CMC) at Seoul National University (SNU). We also thank the Ministry of Education (MOE) and the Creative Research Initiatives Program of the Ministry of Science and Technology (MOST), Korea, for financial support.

JA980912P

(50) Zeolites become hydrophobic as the silicon content in the framework increases.[1,22]

(51) The pore sizes of ZSM-5 and faujasite type zeolite are ~5.5 and 13 Å, respectively. See: Meier, W. M.; Olson, D. H.; Baerlocher, C. *Atlas of Zeolite Structure Type*, 4th ed.; Elsevier: London, 1996.

(52) (a) Sankararaman, S.; Yoon, K. B. Yabe, T.; Kochi, J. K. *J. Am. Chem. Soc*. **1991**, *113*, 1419. (b) Yoon, K. B.; Hubig, S. M.; Kochi, J. K. *J. Phys. Chem*. **1994**, *98*, 3865.

(53) (a) Schlesener, C. J.; Amatore, C.; Kochi, J. K. *J. Am. Chem. Soc*. **1984**, *106*, 3567, 7472. (b) Schlesener, C. J.; Kochi, J. K. *J. Org. Chem*. **1984**, *49*, 3142. (c) Baciocchi, E.; Bietti, M.; Mattioli, M. *J. Org. Chem*. **1993**, *58*, 7106.

(54) (a) Yonemoto, E. H.; Kim, Y. I.; Schmehl, R. H.; Wallin, J. O.; Shoulders, B. A.; Richardson, B. R.; Haw, J. F.; Mallouk, T. E. *J. Am. Chem. Soc*. **1994**, *116*, 10557. (b) Kim, Y. I.; Mallouk, T. E. *J. Phys. Chem*. **1992**, *96*, 2879. (c) Krueger, J. S.; Mayer, J. E.; Mallouk, T. E. *J. Am. Chem. Soc*. **1988**, *110*, 8232. (d) Persaud, L.; Bard, A. J.; Campion, A.; Fox, M. A.; Mallouk, T. E.; Webber, S. E.; White, J. M. *J. Am. Chem. Soc*. **1987**, *109*, 7309.

(55) (a) Borja, M.; Dutta, P. K. *Nature* **1993**, *362*, 43. (b) Dutta, P. K.; Incavo, J. A. *J. Phys. Chem*. **1987**, *91*, 4443. (c) Dutta, P. K.; Turbeville, W. *J. Phys. Chem*. **1992**, *96*, 9410. (d) Dutta, P. K.; Borja, M. *J. Chem. Soc., Chem. Commun*. **1993**, 1568. (e) Ledney, M.; Dutta, P. K. *J. Am. Chem. Soc*. **1995**, *117*, 7687. (f) Dutta, P. K.; Ledney, M. *Prog. Inorg. Chem*. **1977**, *44*, 209.

(56) (a) Ramamurthy, V., Ed. *Photochemistry in Organized and Constrained Media*; VCH: New York, 1991. (b) Holt, S. L., Ed. *Inorganic Reactions in Organized Media*; ACS Symposium Series 177; American Chemical Society: Washington, DC, 1981.

(57) Fukuzumi, S.; Urano, T.; Suenobu, T. *Chem. Commun*. **1996**, 213.

(58) Corma, A.; Fornés, V.; Garcia, H.; Miranda, M. A.; Primo, J.; Sabater, M.-J. *J. Am. Chem. Soc*. **1994**, *116*, 2276.

(59) (a) Rolinson, D. R. *Chem. Rev*. **1990**, *90*, 867. (b) Rolison, D. R. *Stud. Surf. Sci. Catal*. **1994**, *85*, 543.

(60) (a) Calzaferri. G.; Lanz, M.; Li, J. *J. Chem. Soc., Chem. Commun*. **1995**, 1313. (b) Li, J.; Pfanner, K.; Calzaferri, G. *J. Phys. Chem*. **1995**, *99*, 2119. (c) Li, J.; Calzaferri, G. *J. Electroanal. Chem*. **1994**, *377*, 163. (d) Li, J.; Calzaferri, G. *J. Chem. Soc., Chem. Commun*. **1993**, 1430.

(61) (a) Walcarius, A.; Lamberts, L.; Derouane, E. G. *Electrochim. Acta* **1993**, *38*, 2257. (b) Walcarius, A.; Lamberts, L.; Derouane, E. G. *Electrochim. Acta* **1993**, *38*, 2267.

(62) Gemborys. H. A.; Shaw, B. R. *J. Electroanal. Chem. Interfacial Electrochem*. **1986**, *208*, 95.

(63) Grätzel, M., Kalyanasundaram, K., Eds. *Kinetics and Catalysis in Microheterogeneous Systems*; Marcel Dekker: New York, 1991.